Structural study, 31P NMR and europium photoluminescence properties of a new synthetic fillowite-type phosphate: Na3SrMg11(PO4)9

Amal Boukhris, Teycir Ben Hamed, Benoit Glorieux, Mongi Ben Amara

Structural study, ^{31}P NMR and europium photoluminescence properties of a new synthetic fillowite-type phosphate: $Na_3SrMg_{11}(PO_4)_9$

Amal Boukhris[a]*, Teycir Ben Hamed[a], Benoit Glorieux[b], Mongi Ben Amara[a]

[a]*UR : Matériaux Inorganiques, Faculté des Sciences, Université de Monastir, 5019, Monastir - Tunisie*

[b]*Institut de Chimie de la Matière Condensée de Bordeaux, CNRS, Université Bordeaux I, 87, Avenue du Dr. A. Schweitzer, 33608 Pessac-Cedex, France*

*To whom correspondence should be addressed. E-mail: amal.boukhris@yahoo.fr

Abstract

A new phosphate compound, $Na_3SrMg_{11}(PO_4)_9$ was synthesized as single crystals by flux method and as powdered sample by Pechini technique and investigated by X-ray diffraction, ^{31}P NMR and photoluminescence spectroscopies. This compound crystallizes in the rhombohedral space group R $\bar{3}$ and its equivalent hexagonal cell has the following parameters: a = 14.941(1) Å, c = 42.478(2) Å and Z = 12. The structure consisted of MgO_x (x=5,6), NaO_x (x=6,7) and $(Na,Sr)O_x$ (x=8,9) polyhedra which are linked either directly through common corners, edges and faces and by means of the PO_4 tetrahedra via common corners and edges, giving rise to a three-dimensional framework, similar to that of the fillowite-like structure. ^{31}P NMR spectroscopy confirmed the presence of six distinct phosphors sites in the structure. Finally, strontium was partially substitute by divalent europium in order to examine whether this material could be used in optical applications. Optical studies were performed on the $Na_3Sr_{0.98}Eu^{2+}_{0.02}Mg_{11}(PO_4)_9$ compound. The photoluminescence are consistent with the crystal structural and show various properties as a function of the excitation wavelength.

Keywords: Inorganic compounds; Chemical synthesis; X-ray diffraction; Single crystal structure; Nuclear Magnetic Resonance (NMR); Photoluminescence

1. Introduction

The name fillowite relates to a phosphate mineral which has been described by Brush and Dana [1] in the Branchville Connecticut pegmatite and which is well known to occur as an accessory phosphate in rare elements granitic pegmatites. A few numbers of mineral compounds with fillowite structure as $Na_2Ca(Mn_4Mg_2Fe)(PO_4)_6$ [2], $Na_4Ca_4Mg_{21}(PO_4)_{18}$ [3], $Na(Na,Mn)_7Mn_{22}(PO_4)18{\cdot}0.5H_2O$ [4], $Na_{10}(Na,Mn)_7Mn_{43}(PO_4)_{36}$ [5] and $Na_{2.5}Y_{0.5}Mg_7(PO_4)_6$ [6], were described up to date. The classification of these minerals has been established according to the nature of the cation in the M site, from the general formula $Na_2CaM^{2+}{}_7(PO_4)_6$ (M^{2+} = Fe^{2+}, Mn^{2+}, Mg^{2+}) [7]. Indeed, the Mn-rich and the Mg-rich, with chemical compositions $Na_2CaMn_7(PO_4)_6$ and $Na_2CaMg_7(PO_4)_6$, are named fillowite [7] and Chladniite [8], respectively. Johnsomervilleite, $Na_2CaFe_7(PO_4)_6$, is the Fe^{2+}-rich equivalent of fillowite [9], whereas galileiite, $NaFe^{2+}{}_4(PO_4)_3$, corresponds to the johnsommervilleite more rich in Fe^{2+} [10].

The very complex crystal structure of this mineral has been determined by Araki and Moore 1981 with the chemical composition $Na_2CaM^{2+}{}_7(PO_4)_6$ (M^{2+}= Mn, Fe or Mg) and Z = 18. Forty-five none equivalent atoms in the asymmetric unit can be attributed to the very large unit cell of fillowite with a = 15.282(2) and c = 43.507(3) Å. Their atomic arrangement has been described by an hexagonal rod packing [7] and was also considered as a lacunar glaserite type structure like $K_3Na(SO_4)_2$ [11] with lattice parameters approximate $a_F = 3a_G$ et $c_F = 6\ c_G$ [6].

Its complex three-dimensional framework was described in terms of three kinds of rods, called I, II and III, all running along the *c* crystallographic direction. Rods I and II pass through the (*a*, *b*) plane at (0, 0) and (1/3,1/3), respectively and are both consisted by large cations X such as Ca, Na and Mn. Rod III consists of the X cations, T (T = P, S) tetrahedrally coordinated and two types of ordered vacancies, called □(1) and □(2), in the following sequence -T-X-T-X-T-□(1)-T-X-T-X-T-□(2)-.

Optical investigations are used as complementary characterizations. Indeed, the emission and excitation spectra of Eu^{2+} usually consist of broad bands due to parity allowed electric dipole transitions from the lowest band of the $4f^65d^1$excited configuration to the ground state of the $4f^7$ configuration (hereafter 5d→4f). The position of energy levels and consequently the wavelength of excitation and emission bands strongly depend on the nature of the Eu^{2+} surroundings [12].

In this context, the investigation of the system Na_3PO_4-$Mg_3(PO_4)_2$-$Sr_3(PO_4)_2$ led to the synthesis and structural characterizations of a new compound $Na_3SrMg_{11}(PO_4)_9$. Optical properties of its Eu^{2+} doped phase were discussed.

2. Experimental

Single crystals of $Na_3SrMg_{11}(PO_4)_9$ were grown in a flux of sodium molybdate Na_2MoO_4 with an atomic ratio P: Mo = 2:1. A starting mixture of Na_2CO_3, $MgCO_3$, $SrCO_3$, $(NH_4)H_2PO_4$ and $Na_2MoO_4{\cdot}2H_2O$ was dissolved in nitric acid and the obtained solution was evaporated to dryness. The dry residue was transferred into a platinum crucible and then heated in stages up to 473, 673 and 873 K for 24 h at each stage.

After being, the sample melted for 1 h at 1273 K and then cooled down to room temperature with a 10 K/h. The final product was washes with warm water to dissolve the flux and quasi-spherical colorless crystals were extract from this mixture. Their elementary analysis by ICP performed by "Spectroflame modula ICP" showed the exclusive presence of Na, Sr, Mg and P in weight ratios Na:Sr:Mg:P≈5.26:7.01:20.81:21.4, close to those Na:Sr:Mg:P≈5.39:6.85:20.91:21.8 calculated for the $Na_3SrMg_{11}(PO_4)_9$ formula.

This compound was also synthesized in the powder form by the Pechini method [13]. The starting materials include $NaCO_3$, $MgCO_3$, $SrCO_3$ (Eu_2O_3 for doped phases), analytical reagent grade HNO_3, citric acid, and ethylene glycol. Firstly, $NaCO_3$ and $MgCO_3$ were dissolved in diluted nitric acid. Secondly, $SrCO_3$ (Eu_2O_3) and $(NH_4)H_2PO_4$ were dissolved with citric acid and ethylene glycol were added to the obtained solution. The aqueous solution was kept at 333 K for 8 h under continuous stirring. At last, the transparent gel was heated at 423 K, and the brown resin was obtained. This resin was fired at different temperatures 473, 673,873 and1073 K with intermediate grinding.

The same method was used to prepare the europium doped phase: $Na_3Sr_{0.98}Eu^{2+}_{0.02}Mg_{11}(PO_4)_9$. Doping by divalent europium was performed according to the following mechanism: Eu^{2+} = Sr^{2+} and the final thermal treatment were performed under $Ar–H_2$ atmosphere.

The structure of $Na_3SrMg_{11}(PO_4)_9$ was determined by single crystal X-ray diffraction using a spherical crystal with dimensions 0.18×0.18×0.20 mm^3. Data were collected by an Enraf-Nonius CAD4 diffractometer using a graphite mono-chromated MoKα radiation (λ = 0.71073 Å). The unit cell parameters and the orientation matrix were determined on the basis of 25 intense reflections in the range $8.72^o \leq \theta \leq 10^o$. A total of 6520 reflections were collected using the ω/2θ scan mode. Only 4939 reflections were considered observed

according to the statistic criterion ($F_0 > 4\sigma(F_0)$). The intensity data were corrected for the Lorentz and polarization effects. Based on systematic absences, statistic of intensity distribution and refinement of the structure, the space group was determined to be $R\bar{3}$. The structure was solved by direct methods [14] which revealed the position of strontium atoms. The remaining atomic positions were located by Fourier synthesis alternating with least squares refinement based on F^2 (SHELXL-97) [15] (Sheldrick 1997). Finally, refinement including all atomic coordinates and anisotropic thermal parameters converged at $R_1 = 0.044$ and $wR_2 = 0.10$ for the observed reflections.

^{31}P-NMR spectra were recorded with a Bruker 500 spectrometer (B = 7.1 T) equipped with a 4 mm probe head, operating at a ^{31}P resonating frequency of 121.49 MHz and a rotor spin rate of 10 kHz. 4096 data points are collected over an acquisition time of 65 ms, an inter-acquisition delay of 60 s and a number of scans of 24. The MAS ^{31}P-NMR spectra were acquired with a simple sequence zg pulse of 5 µs and an attenuation level of 10 dB. The ^{31}P chemical shifts were referenced to 85% aqueous H_3PO_4. The spectrum was deconvoluted using the DMfit program [16].

Excitation and emission measurements were performed using a spectrofluorimeter SPEX FL212. The light beam produced by a 450 W xenon lamp, passes through an excitation double monochromator in order to irradiate the powder sample. The emitted light selected with an emission double monochromator, is recorded by a thermoelectrically cooled photomultiplier tube.

3. Results and discussion

3.1. X-Ray Diffraction results

The purity of powder form phases was checked from an examination of their powder X-ray diagram (Fig. 1).

Crystal data, experimental conditions for data collection and refinement parameters are given in Table 1. Final atomic coordinates and equivalent isotropic temperature factors are reported in Table 2.

3.2. Description of the structure

The crystal data for the $Na_3SrMg_{11}(PO_4)_9$ structure as well as its projection along c-axis (Fig. 2) show an isotypism with those of the fillowite-like compounds [7]. This structure consists of six PO_4 tetrahedra and 15 cationic sites with coordination number varying between 5 and 9. Various polyhedra are distinguished: seven MgO_6 octahedra, four MgO_5 polyhedra,

two polyhedra NaO_x (x = 6, 7) and two polyhedra $(Na,Sr)O_x$ (x = 8,9) containing a statistical distribution of sodium and strontium.

According to the structural model proposed by Araki & Moore [7], this structure can be described, on the basis of three types of rods I, II and III running along the c axis.

Rod I (Fig. 3) consists of units of face-sharing $Mg(i)O_6$ (i = 3, 4, 5), $Na(1)O_6$ and $(Sr,Na)O_9$ polyhedra. Such units are separated by $Mg(1)O_6$ and $Mg(2)O_6$ octahedra leading to a staking sequence of :

[Mg(1)—Mg(3)—Na(1)—(SrNa)(1)—Mg(4)—Mg(5)—Mg(2)—Mg(5)—Mg(4)—(SrNa)(1)—Na(1)—Mg(3)]$_\infty$

Rod II (Fig. 2) consists of corner- and edge-sharing $Mg(11)O_6$, $Mg(8)O_5$, $Na(2)O_7$, and $(Sr,Na)O_8$ polyhedra which form a sequence of : [SrNa(2)—Mg(11)—Na(2)—Mg(8)]$_\infty$

Rod III (Figure 3) consists of units of corner-sharing PO_4, $Mg(i)O_5$ (i= 6,7, 9) and $Mg(10)O_6$ polyhedra. These units are separated by ordered vacancies $\square_1$ and $\square_2$ to form a sequence of:

[P(2)—Mg(9)—P(3)—Mg(7)—P(6)—□—P(1)—Mg(10)—P(4)—Mg(6)—P(5) —□]$_\infty$

Figure 4 shows the six phosphorus environment within a radius of 5 Å. Table 3 gives main interatomic distances in $Na_3SrMg_{11}(PO_4)_9$. Magnesium occupies eleven crystallographically independent sites. Mg(6) to Mg(9) are five-coordinated with Mg–O distances varying from 1.972(1) to 2.255(1) Å. Their average values (from 2.053 to 2.093 Å) are close to that 2.08 Ǻ reported for the five coordinated Mg^{2+} ion in $NaMg_4(PO_4)_3$ [17]. The other magnesium sites are octahedral with Mg–O average distances ranging from 2.059(1) to 2.148(1) Å, in a good agreement with that (2.14 Å) observed for hexacoordinated Mg^{2+} ions in $Mg_3(PO_4)_2$ [18]. The six PO_4 tetrahedra have an average distances <P–O> between 1.534 (1) and 1.539 (2) Å consistent with 1.537 Å, predicted by Bauer for the monophosphate groups [19]. The environments of the Sr^{2+} and Na^+ sites were determined assuming maxima cation-oxygen distances L_{max} of 3.27 Ǻ and 3.13 Ǻ, respectively, as suggested by Donnay and Allmann [20]. The two (Na,Sr) sites are 8 and 9 coordinated with (Na,Sr)–O distances in the range of 2.404(2)-2.811(1) Å, leading to an average distance of <Sr,Na(1)–O> = 2.643(1) and <Sr,Na(2)–O> = 2.619(1). The Na(1) and Na(2) environments are consisted by 6 and 7 oxygen atoms with average distances <Na(1)–O> = 2.449(1) Å and <Na(2)–O> = 2.527(1).

$Na_3SrMg_{11}(PO_4)_9$ as is the case of $Na_{2.5}Mg_7Y_{0.5}(PO_4)_6$ [6], displays strong similarities with the Mg-rich fillowite $Na_4Ca_4Mg_{21}(PO_4)_{18}$ reported by Domanskii et al. [3] but with some

differences as shown in Table 4. First, the octahedral sites occupied by calcium in the $Na_4Ca_4Mg_{21}(PO_4)_{18}$ structure are occupied by magnesium (Mg(1) and Mg(2)) in the present structure and by yttrium (Y(1) and Y(2)) in $Na_{2.5}Mg_7Y_{0.5}(PO_4)_6$. Second, the cationic site occupied by calcium (Ca(1)) in $Na_4Ca_4Mg_{21}(PO_4)_{18}$ is occupied statistically by strontium and sodium in $Na_3SrMg_{11}(PO_4)_9$ and by yttrium and sodium in $Na_{2.5}Mg_7Y_{0.5}(PO_4)_6$ structure. Third, the sodium site (Na(2)) in Ca- and Y-fillowite is occupied statistically by strontium and sodium in the present structure. Finally, the sodium site, Na(1) for $Na_3SrMg_{11}(PO_4)_9$ and Na(3) for $Na_{2.5}Mg_7Y_{0.5}(PO_4)_6$, is unoccupied in $Na_4Ca_4Mg_{21}(PO_4)_{18}$ structure.

3.3. ^{31}P NMR analysis

A ^{31}P NMR spectroscopy study was undertaken to confirm the number of phosphorus environments in $Na_3SrMg_{11}(PO_4)_9$ structure. The spectrum, shown in Fig. 5, consists of a broad and complex signal arising from the overlap of several peaks in an area of -2.5 to 7 ppm, in a good agreement with the values previously reported for other monophosphates [21, 22, 23]. Its fit revealed six resonances at 6.92; 3.68; 2.8; 1.77; -0.38 and -2.44 ppm, in accordance with the results of structural analysis who showed the presence of 6 phosphor tetrahedra (Fig. 4). The various position, from -2.5 to 7ppm are due to the influence of the environment surrounding the P cations [24-26]. This can be related to the covalence degree of P–O bond. In fact, when the antagonist bond (cation–oxygen) become more covalent, the covalence of the P–O bond decreases involving an evolution of the chemical shift to the positive values.

In the $Na_3SrMg_{11}(PO_4)_9$ structure, all the Mg–O distances are less than 2.2 Å while those of sodium and strontium are larger. Therefore, it can be considered that the first cationic shells around the phosphate groups are formed by only the Mg ions while sodium and strontium form the second cationic shells. Consequently, the variation of ^{31}P chemical shift is mainly due to a slight decrease of the covalent caracter of Mg–(OPO_3). So, the decrease of the mean distances <Mg-O> induces an evolution of ^{31}P chemical shift to the positive values. An attempt of assignment of NMR signals to the different phosphate groups is then proposed (Table 5). Figure 6 shows the correlation between the chemical shift and the electric field strength Z/a^2 [27,28] with Z: the valence and a: the mean internuclear distance <Mg–O> within the first cationic shells of each phosphate group.

3.4. Photoluminescence study

The title compound doped with divalent europium is analyzed by photoluminescence. The excitation and emission spectra for the $Na_3Sr_{0.98}Eu^{2+}_{0.02}Mg_{11}(PO_4)_9$ phase are shown in Fig. 7.

The two excitation spectra are recorded for emission at λ_{em} = 430 nm and 475. Each spectrum comprises two broad bands related to the 4f-5d transition of Eu^{2+}, meaning that the divalent europium is located in more than one site. Some defect, especially at high energy, might be also revealed in these bands. This situation is reminiscent of those observed in the two compounds doped with divalent europium $Na_2MMg(PO_4)_2$ with M = Sr and Ba [21,29]. The ionic radius of Sr^{2+} (r_i= 1.31 Å) and Eu^{2+} (r_i= 1.3 Å) are similar for the same coordination number IX. It can therefore be estimated that in $Na_3Sr_{0.98}Eu^{2+}_{0.02}Mg_{11}(PO_4)_9$, divalent europium occupies the two sites of strontium (Sr,Na)(1) and (Sr,Na)(2) which have high coordination numbers, 9 and 8 respectively. The position of these bands, and more specifically the Stokes Shift [30] (i.e. difference between excitation and emission band), are related to the crystal field of the polyhedral surrounding the divalent europium cation.

Under the 220 and 350 nm excitations, the emission spectra consist of a broad and asymmetrical band centered in the blue-purple range. These bands can not be fitted by only one Gaussian each. The two emission spectra can be deconvoluted into two Gaussian bands, centred at about 425, 476 nm and 423, 449 nm for the 220 and 350 nm excitations, respectively as shown in Fig. 8.

Under the 220 nm excitation, the emission spectrum shows additional peaks above 575 nm assigned to the $^5D_0 \rightarrow ^7F_J$ transitions of Eu^{3+} [31, 32]. This indicates the presence of europium unreduced in this phase even after variety of heat treatments adopted during synthesis. Various syntheses were performed to obtain compounds showing emission spectra without any peaks relevant of trivalent europium. The treatement at 473 K, 673K, 873 K, and 1073 K were performed under Ar-H_2 atmosphere, during extended period of time, from 8 h to 72 h. The emission signal of trivalent europium did always appear in the photoluminescence measurement.

The emission peaks related to the trivalent europium, situated between 582 and 600 nm are due to the magnetic dipole transition $^5D_0 \rightarrow ^7F_1$ and the emission bands at about 600–630 nm, are due to the $^5D_0 \rightarrow ^7F_2$ electric dipole transition. The ratio $\frac{I_{^5D_0 \rightarrow ^7F_2}}{I_{^5D_0 \rightarrow ^7F_1}}$ is then used to characterize the centro-symmetry of the europium site [33]. The europium located on an inversion center induces the most intense $^5D_0 \rightarrow ^7F_1$ transition.

The emission under excitation at 220 nm shows that $^5D_0 \rightarrow {}^7F_1$ transitions are more intense than those of $^5D_0 \rightarrow {}^7F_2$, implying that Eu^{3+} is in a centrosymmetric site. Moreover, the peaks related to $^5D_0 \rightarrow {}^7F_1$ transitions are quite compact, indicating a low crystal field surrounding the europium cations [34, 35]. Therefore, it is suggested that the trivalent europium is located in one of the magnesium site having a centrosymmetric characteristic. Looking at the table 3, it can correspond to Mg(1) and Mg(2) sites.

The relevance of trivalent europium can be explained by the substitution of Eu^{3+} to Mg^{2+} in the two sites of symmetry (-3) favourable to rare earth ions of small size, such as the case of Y^{3+} in the structure of $Na_{2.5}Mg_7Y_{0.5}(PO_4)_6$ [6].

Regarding the luminescence of divalent europium, the corresponding spectra shows three bands, as seen in the deconvolutions in the Figure 8, centered at 424 nm, 449 nm and 476 nm. It means that Eu^{2+} ions occupy three different sites in the fillowite structure. Two sites corresponding to the two strontium sites are expected in agreement with the analysis of excitation spectra and the crystallographic results. The third one might be assigned to the eventual insertion of Eu^{2+} in the sodium site as it has been observed for $Na_2BaMg(PO_4)_2$: Eu^{2+} [29]. The position of the bands, in relation with the crystal field surrounding the divalent europium cation, some attempts to link the emission bands to the localization of divalent europium in the structure are performed.

The band centered at 424 nm might correspond to the europium localized in the sodium site ($Na(1)O_6$ or $Na(2)O_7$). The band centered at 449 nm might correspond to the europium localized in the strontium site of the $(Sr,Na)(2)O_8$ polyhedron and the band centered at 476 nm might correspond to the europium localized in the strontium site of the $(Sr,Na)(1)O_9$ polyhedron.

Finally, the color coordinates of the powder sample doped with divalent europium, excited at 220 nm are ($x = 0.154$, $y = 0.059$) in the CIE 1931 color space chromatic diagram [36], corresponding to a deep blue color. For an excitation at 350 nm, the color coordinates are ($x = 0.235$, $y = 0.267$) corresponding to a turquoise color (Fig. 9).

It appears that this fillowite compound shows various optical properties by changing the excitation wavelength, from deep blue to turquoise luminescence, due to the various position of europium in the structure. This characteristic could lead to various applications where the incident light, targeting the phosphor, is adjustable.

4. Conclusion

$Na_3SrMg_{11}(PO_4)_9$ was synthesized as single crystals by the flux method and as a powdered sample by the Pechini technique. Its structure related to the fillowite type can be described according to Moore and Araki, on the basis of three types of rods parallel to the c axis: I, II and III. The ^{31}P NMR spectrum was consistent with the structural study predicting the presence of six types of site for the phosphorus. The divalent europium was used to analyze the effects of the sample composition on the blue luminescence for its eventual integration in optical applications.

Acknowledgment

This work was supported by the Ministry of Higher Education, Scientific Research and Information Technology and Communication (Tunisia) and the national Center for Scientific Research (France): Project (DGRS‑CNRS) (14/R1202).

References

[1] G.J. Brush, E.S. Dana, On a new remarkable mineral locality in Fairfield County, Connecticut; with description of several new species occurring there, Am J Sci. 116 (1878) 33-46.

[2] Ma. Zhesheng, Shi. Nicheng, Ye. Danian, Mineralogy and crystal structure determination of Mg-fillowite, Sci China Ser D. 48(5) (2005) 635-646.

[3] A. I. Domanskii, YU. I. Smolin, YU. F. Shepelev, J. Majling, Determination of crystal structure of triple magnesium calcium sodium orthophosphate $Mg_{21}Ca_4Na_4(PO_4)_{18}$, Sov Phys Crystallogr. 27 (1983) 535-537.

[4] P. Keller, F. Hatert, F. Lissner, T. Schleid, A. M. Fransolet, Hydrothermal synthesis and crystal structure of $Na(Na,Mn)_7Mn_{22}(PO_4)_{18}\cdot 0.5H_2O$, a new compound of fillowite structure type, Eur J Mineral. 18 (2006) 765-774.

[5] F. Harter, P. Keller, F. Lissner, T. Schleid, $Na_{10}(Na,Mn)_7Mn_{43}(PO_4)_{36}$: a new synthetic fillowite-type phosphate, Acta Crystallogr. C 65 (2009) 52-53.

[6] H. Jerbi, M. Hidouri, M. Ben Amara, Synthesis and structural characterization of a new yttrium phosphate: $Na_{2.5}Y_{0.5}Mg_7(PO_4)_6$ with fillowite-type structure, J Rare Earth. 28 (2010) 481-487.

[7] T. Araki, P.B. Moore, Fillowite, $Na_2Ca(Mn,Fe)^{2+}_7(PO_4)_6$: its crystal structure, Am Mineral. 66 (1981) 827-842.

[8] T.J. McCoy, I.M. Steele, K. Keil, B.F. Leonard, M. Endreb, Chladniite, $Na_2CaMg_7(PO_4)_6$: A new mineral from the Carlton (IIICD) iron meteorite, Am Mineral. 79 (1994) 375-380.

[9] A. Livingstone, Johnsomervilleite, a new transition-metal phosphate mineral from the Loch Quoid area, Scontland, Mineral Mag. 43 (1980) 833-836.

[10] E.J. Olsen, I.M. Steele, Galileiite: a new meteoritic phosphate mineral, Meteorit Planet Sci. 32 (1997) 155-156.

[11] K. Okado, J. Ossaka, Structures of potassium sodium sulphate and tripotassium sodium disulphate, Acta Crystallogr. B 36 (1980) 919-921.

[12] S.H.M. Poort, W.P. Blokpoel, G. Blasse, Luminescence of Eu^{2+} in barium and strontium aluminate and gallate, Chem Mater. 7 (1995) 1547-1551.

[13] M.P. Pechini, Method of preparing lead and alkaline earth titanates and niobates and coating method using the same to, US form a capacitor Patent, 3 (1967) 697.

[14] A. Altomare, G. Cascarano, C. Giacovazzo, A. Guagliardi, Completion and refinement of crystal structures with SIR92, J Appl Crystallogr. 26 (1993) 343-350.

[15] G.M. Sheldrick, SHELXL97, A Program for the Solution of the Crystal Structure. Göttingen: University of Göttingen (1997).

[16] D. Massiot, F. Fayon, M. Capron, I. King, S. Le Clavé, B. Alonso, J.O. Durand, B. Bujoli, Z. Gan, G. Hoatson, Modelling one-and two-dimensional solid-state NMR spectra, Magn Reson Chem. 40 (2002) 70-76.

[17] M. Ben Amara, M. Vlasse, R. Olazcuaga, J. Le Flem, P. Hagenmuler, Structure de l'orthophosphate triple de magnésium et de sodium, $NaMg_4(PO_4)_3$, Acta Crystallogr. C 39 (1983) 936-939.

[18] S. Jaulmes, A. Elfkir, M. Quarton, F. Brunet, C. Chopin, Structure cristalline de la phase haute température et haute pression de $Mg_3(PO_4)_2$, J Solid State Chem. 129 (1997) 341-345.

[19] W.H. Baur, The geometry of polyhedral distortions. Predictive relationships for the phosphate group, Acta Crystallogr. B 30 (1974) 1195-1215.

[20] G. Donnay, R. Allmann, How to recognize O^{2-}, OH^- and H_2O in crystal structures determined by X-rays, Am Mineral. 55 (1970) 1003-1015.

[21] A. Boukhris, M. Hidouri, B. Glorieux, M. Ben Amara, Correlation between structure and photoluminescence of the europium doped glaserite-type phosphate $Na_2SrMg(PO_4)_2$, Mater Chem Phys. 137 (2012) 26-33.

[22] R.J.B. Jakeman, A.K. Cheetham, Combined single-crystal X-ray diffraction and magic angle spinning NMR study of α-$CaZn_2(PO_4)$, J Am Chem Soc. 110 (1988) 1140-1143.

[23] B. Louati, F. Hlel, K. Guidara, M. Gargouri, Analysis of the effects of thermal treatment on $CaHPO_4$ by ^{31}P NMR spectroscopy, J Alloy Compd. 394 (2005) 13-18.

[24] G.L. Turner, K.A. Smith, R.J. Kirkpatrick, E. Old field, Structure and cation effects on phosphorus-31 NMR chemical shifts and chemical shift anisotropies of orthophosphates. J Magn Res. 70 (1986) 408-415.

[25] A.K. Cheetham, N.J. Clayden, C.M. Dobson, R.J.B. Jakeman, Correlations between ^{31}P NMR Chemical Shifts and Structural Parameters in Crystalline Inorganic Phosphates, J Chem Soc Chem Commun. 3 (1986) 195-197.

[26] I. Abrahams, A. Ahmed, C. Christopher, J. Groombridge, Cation distribution in cubic $NaM(PO_3)_3$ (M = Mg or Zn) using X-ray powder diffraction and solid state NMR, Chem Soc Dalton Trans. 2 (2000) 155-160.

[27] R.T Sanderson, Polar Covalence, Academic Press, New York: 40 (1983).

[28] M. Colmont, L. Delevoye, E.M. Ketatni, L. Montagne, O. Mentré, Structural and ^{31}P NMR investigation of $Bi(MM')_2PO_6$ statistic solid solutions: Deconvolution of lattice constraints and cationic influences, J Solid State Chem. 179 (2006) 2111-2119.

[29] A. Boukhris, M. Hidouri, B. Glorieux, M. Ben Amara, $Na_2BaMg(PO_4)_2$: synthesis, crystal structure and europium photoluminescence properties, J Rare Earth. 31 (2013) 849-856.

[30] G. Blasse, A. Bril, Investigation of Some Ce^{3+}Activated Phosphors, J Chem Phys. 47 (1967) 5442-5443.

[31] D. Vander Voort, G.J. Dirksen, G. Blasé, Luminescence study of Eu^{3+}–O^{2-} associates in fluorides: CaF_2, $RbCdF_3$and $RbCaF_3$, J Phys Chem Solids. 53 (1992) 219-225.

[32] C. Cascales, E. Antic-Fidancev, M. Lemaître-Blaise, P. Porcher, Spectroscopic properties of Eu^{3+} in lanthanum chlorotungstates, J Solid State Chem. 89 (1990) 118-122.

[33] P.A.M. Berdowski, G. Blasse, Luminescence and energy transfer in a highly symmetrical system: $Eu_2Ti_2O_7$, J Solid State Chem. 62 (1986) 317-327.

[34] G. Blasse, A. Bril, W-C. Nieuwpoort, On the Eu^{3+} fluorescence in mixed metal oxides. Part I. The crystal structure sensitivity of the intensity ratio of electric and magnetic dipole emission, J Phys Chem Solids. 27 (1966) 1587-1592.

[35] C. Görller-Walrand, K. Binnemans, Rationalization of Crystal-Field Parametrization in Handbook on the Physics and Chemistry of Rare Earths, K.A. Gschneidner Jr and L. Eyring, Elsevier Science, Amsterdam 23 (1996) 121-283.

[36] R.W.G. Hunt, Measuring Colour. Foutain Press, England, (1988) 740-749.

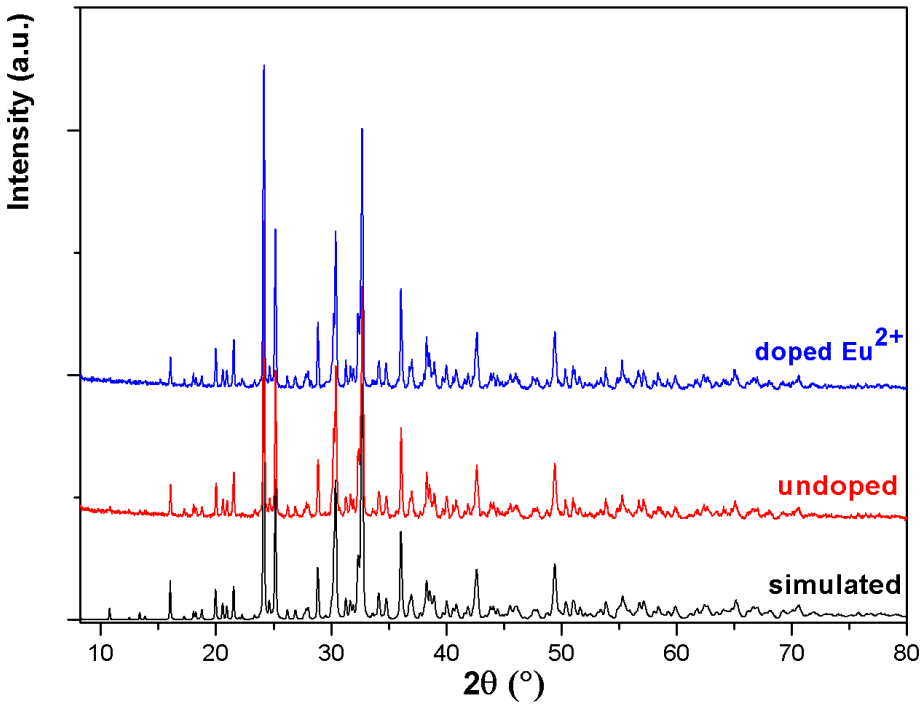

Figure 1 Observed X-ray patterns for $Na_3SrMg_{11}(PO_4)_9$ (undoped) and its doped Eu^{2+} phase compared to the simulated spectra.

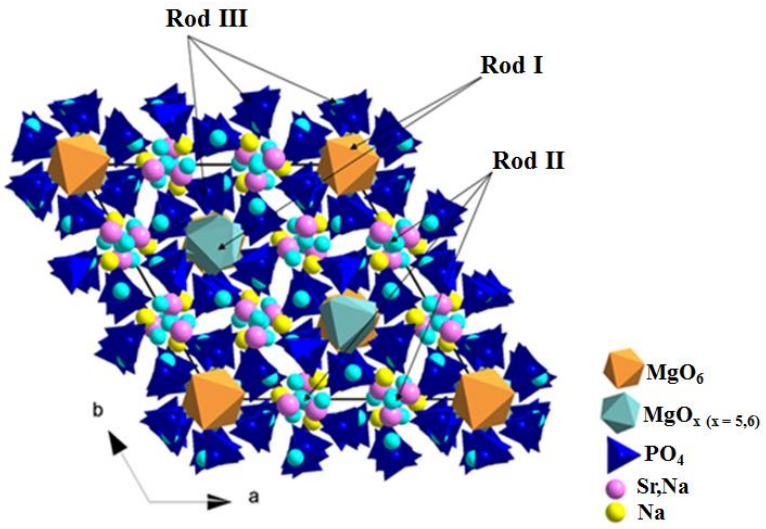

Figure 2 Projection along the [001] direction of the $Na_3SrMg_{11}(PO_4)_9$ structure showing the hexagonal rod packing.

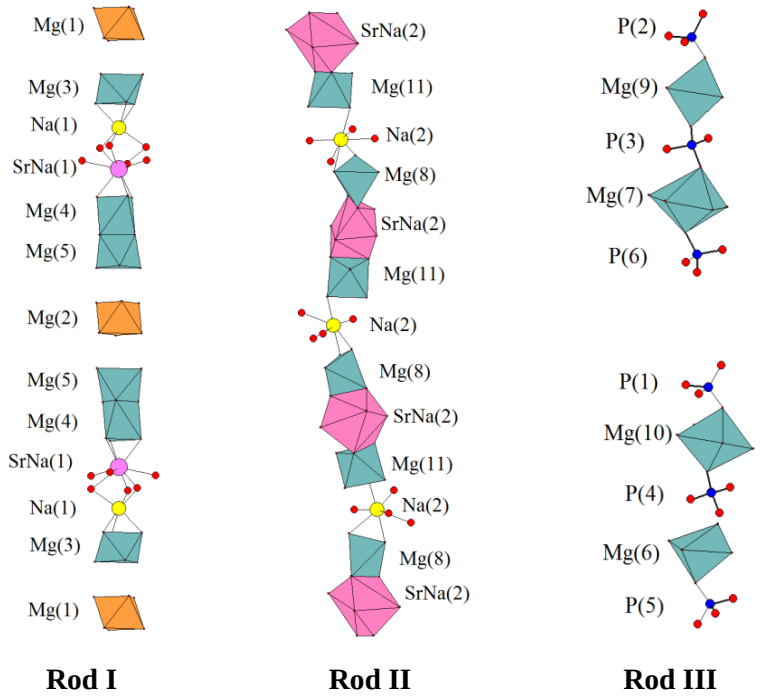

Figure 3 Rods I, II and III in $Na_3SrMg_{11}(PO_4)_9$.

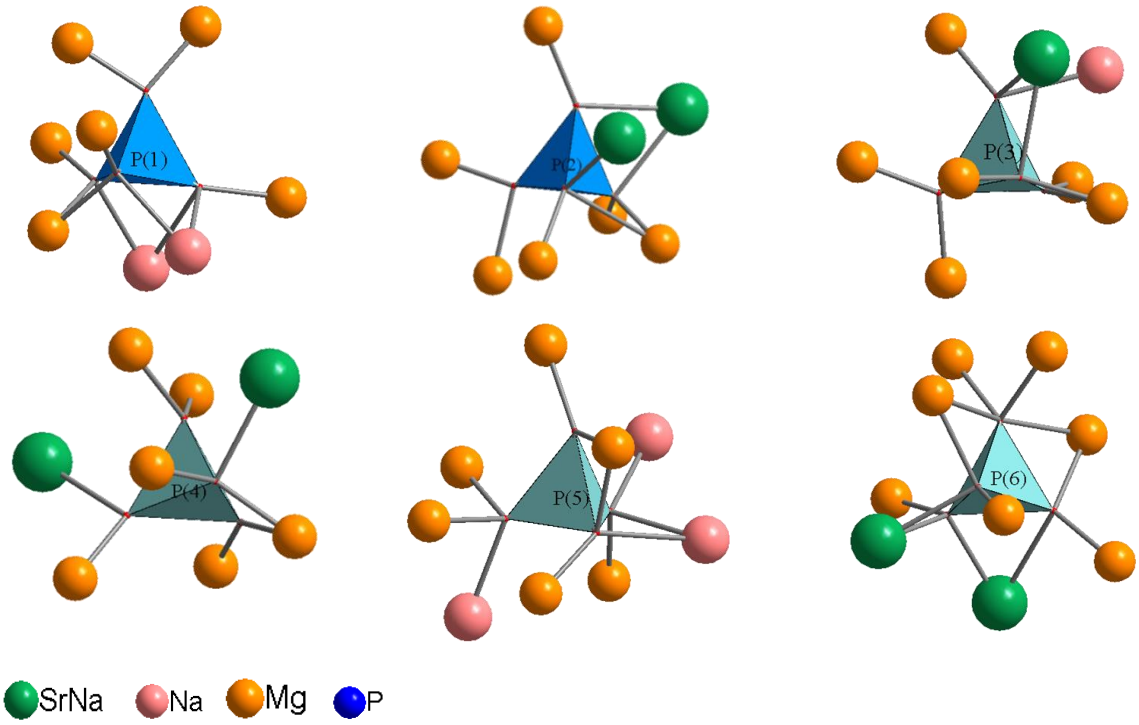

Figure 4 Environments of the six phosphorus sites in $Na_3SrMg_{11}(PO_4)_9$.

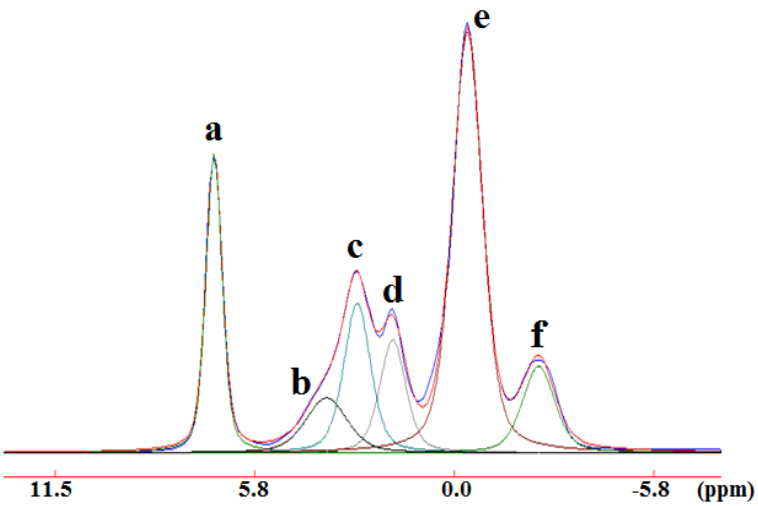

Signals	Position (ppm)	FWHM	Amplitude
a	6.92	0.55	690
b	3.68	1.41	130
c	2.80	0.91	350
d	1.77	0.89	260
e	-0.38	1.02	980
f	-2.44	1.10	200

Figure 5 ^{31}P NMR spectrum of $Na_3SrMg_{11}(PO_4)_9$; Table summarizes the main data deconvolution.

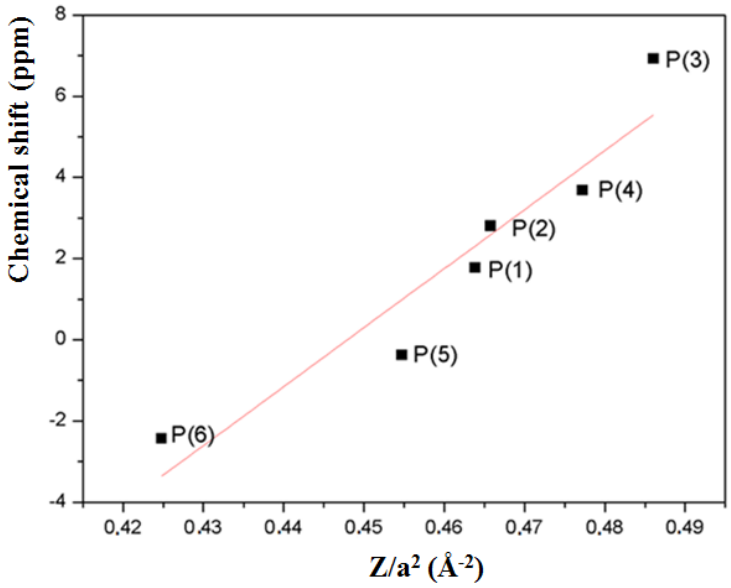

Figure 6 Variation of the experimental ^{31}P chemical shift versus Z/a^2.

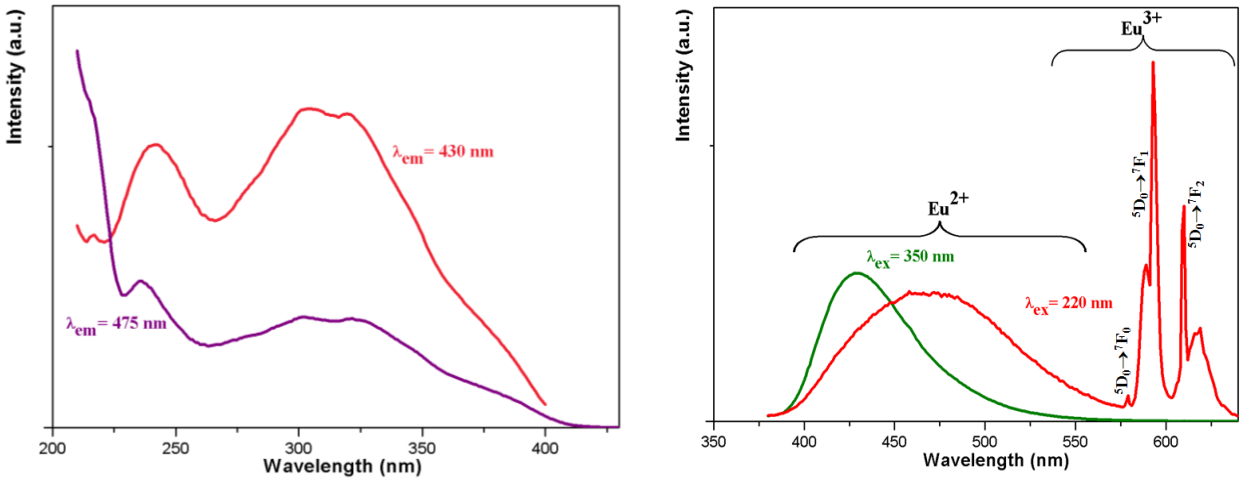

Excitation spectra Emission spectra

Figure 7 Photoluminescence spectra of $Na_3Sr_{0.98}Eu^{2+}_{0.02}Mg_{11}(PO_4)_9$.

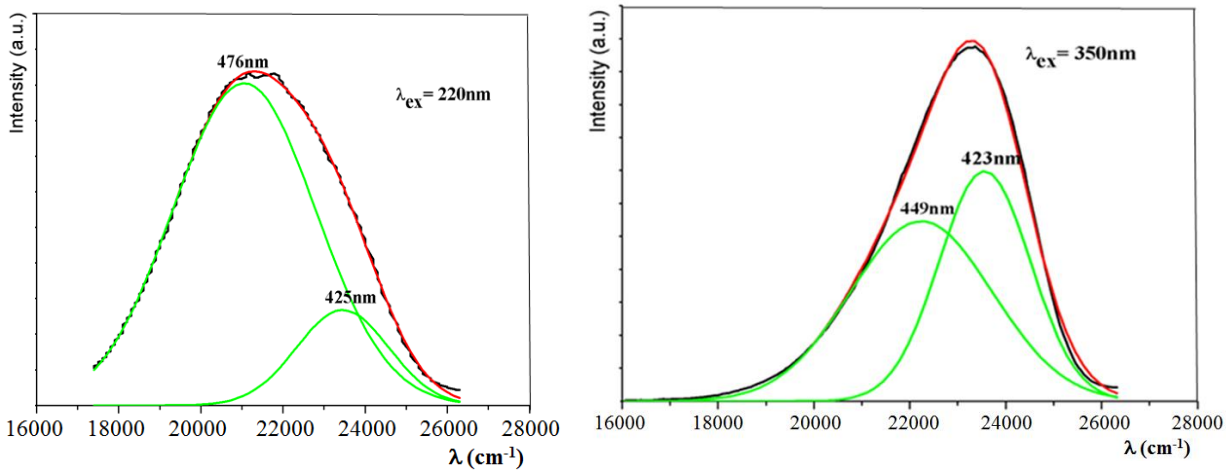

Figure 8 Emission spectra of $Na_3Sr_{0.98}Eu^{2+}_{0.02}Mg_{11}(PO_4)_9$ deconvoluted in two Gaussian components.

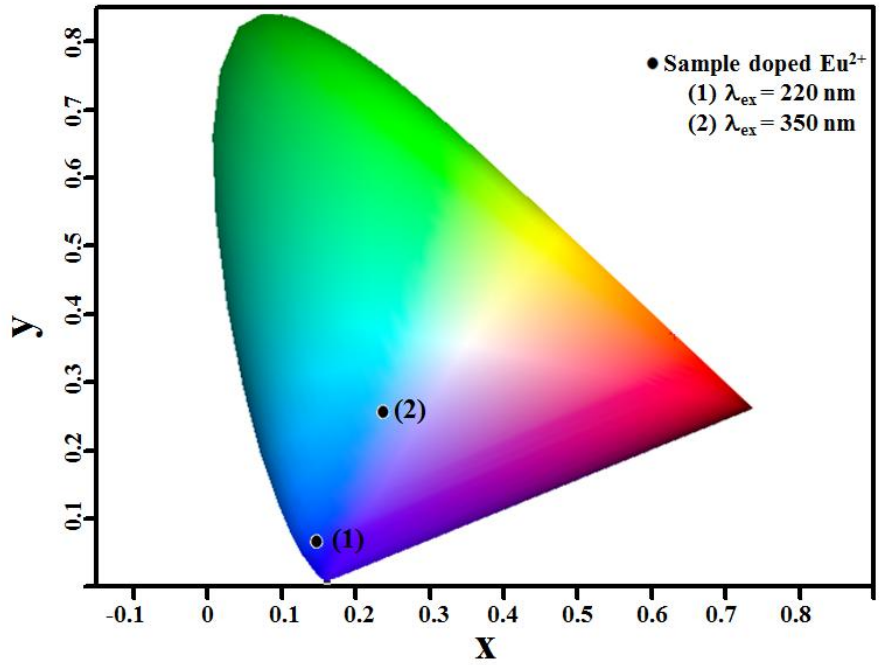

Figure 9 CIE chromaticity positions of $Na_3SrMg_{11}(PO_4)_9$: Eu^{2+}.

Table 1: Crystal data, experimental conditions for data collection and refinement parameters

Crystal data	
Chemical formula	$Na_3SrMg_{11}(PO_4)_9$
Space group	R $\overline{3}$
a (Å)	14.941(1)
c (Å)	42.478(2)
Z	12
ρ_{cal} (g.cm^{-3})	3.10
Intensity measurements	
Crystal dimensions (mm)	0.18 × 0.18 × 0.20
Apparatus	CAD4(Enraf –Nonius)
λ(MoK$_\alpha$) (Å)	0.56085
Monochromator	Graphite
μ (mm^{-1})	1.57
Scan mode	ω/2θ
$2\theta_{max}$	25°
Reflections ; R_{int}	6520 ; 0,033
Observed reflections (F_0>4σ(F_0))	4939
Indices	0<h<19,0<k<19, -63<l< 63
F(000)	7512
Structure resolution and refinement	
Intensity correction	Lorentz and polarization
Absorption correction	None
Resolution method	Direct method
Agreement factors (F_0>4σ(F_0)) :	R_1 = 0.044 ; WR_2 = 0.10 ; S = 1.030
Number of refined parameters	367

Weighting scheme	$w = 1/[\sigma^2(F_0^2) + 0.0672P)^2 + 0.0000P]$ where $P = (F_0^2 + 2F_c^2)/3$
$(\Delta\rho)_{max, min}$ (e.Å^{-3})	1.22; -0.98

Table 2: Atomic position and equivalent thermal parameters U_{eq}(Å^2) for $Na_3SrMg_{11}(PO_4)_9$

Atom	*Occupation*	*x (σ)*	*y (σ)*	*z (σ)*	*U_{eq} (σ)**
(Sr,Na)(1)	0.160(2); 0.840(1)	0	0	0.2472(4)	0.0183(4)
(Sr,Na)(2)	0.613(1); 0.387(2)	0.2887(2)	0.2638(3)	-0.0009(2)	0.0146(1)
Na(1)	1	0	0	0.177(2)	0.0223(5)
Na(2)		0.3196(2)	-0.0932(1)	0.1685(3)	0.0209(3)
Mg(1)	1	0	0	0	0.0097(5)
Mg(2)		0	0	1/2	0.0086(4)
Mg(3)		0	0	0.1042(4)	0.0075(3)
Mg(4)	1	0	0	0.3244(4)	0.0075(3)
Mg(5)		0	0	0.3967(2)	0.0075(3)
Mg(6)		-0.0791(2)	0.4266(2)	0.1233(2)	0.015(2)
Mg(7)		-0.1788(9)	0.2490(2)	0.0522(3)	0.0122(2)
Mg(8)		0.0668(8)	0.3275(8)	0.0864(2)	0.0089(1)
Mg(9)		-0.1120(8)	0.1067(8)	0.1330(3)	0.0107(2)
Mg(10)		0.4613(2)	0.5732(9)	0.0393(2)	0.0111(2)
Mg(11)		-0.0030(2)	0.3221(8)	-0.0824(2)	0.0087(1)
P(1)		0.1291(6)	0.5579(6)	0.1110(2)	0.0059(1)
O(11)		0.1965(2)	0.6008(1)	0.1397(5)	0.0122(4)
O(12)		0.1914(2)	0.5873(1)	0.0802(2)	0.0089(4)
O(13)		0.0441(1)	0.5882(1)	0.1101(5)	0.0099(4)
O(14)		0.0644(2)	0.4376(1)	0.1126(5)	0.0097(4)
P(2)		-0.0830(2)	0.1132(6)	0.0557(2)	0.0067(1)
O(21)		-0.0282(1)	0.1046(2)	0.0270(5)	0.0151(4)
O(22)		-0.0510(2)	0.0874(2)	0.0870(5)	0.0141(4)
O(23)		-0.2001(1)	0.0499(2)	0.0522(5)	0.0145(4)
O(24)		-0.0536(1)	0.2304(1)	0.0588(5)	0.0094(4)
P(3)		0.2067(6)	0.4462(6)	-0.1235(2)	0.0071(1)
O(31)	1	0.1908(2)	0.5395(1)	-0.1235(5)	0.0129(4)
O(32)		0.2488(2)	0.4357(2)	-0.1548(5)	0.0172(5)
O(33)		0.2909(1)	0.4645(1)	-0.0989(5)	0.0111(4)
O(34)		0.1063(1)	0.3438(1)	-0.1158(5)	0.0096(4)
P(4)		0.1166(6)	0.5352(6)	-0.0382(2)	0.0068(1)
O(41)		0.0954(1)	0.4950(1)	-0.0045(5)	0.0116(4)
O(42)		0.1295(1)	0.4578(1)	-0.0587(5)	0.0113(4)
O(43)		0.0328(1)	0.5559(1)	-0.0511(5)	0.0118(4)
O(44)		0.2172(1)	0.6418(2)	-0.0392(5)	0.0096(4)
P(5)		0.1170(6)	0.2420(2)	0.1344(2)	0.0070(1)
O(51)		0.1737(1)	0.2998(1)	0.1640(5)	0.0109(4)
O(52)		0.1789(2)	0.2964(1)	0.1045(5)	0.0106(4)
O(53)		0.0905(1)	0.1279(1)	0.1358(5)	0.0096(4)
O(54)		0.0151(1)	0.2442(2)	0.1312(2)	0.0099(4)
P(6)		0.2460(2)	0.4368(6)	0.0285(2)	0.0064(2)
O(61)		0.3223(1)	0.4123(1)	0.0449(5)	0.0105(4)
O(62)		0.2203(2)	0.3858(1)	-0.0041(2)	0.0091(4)
O(63)		0.1453(1)	0.4016(1)	0.0468(5)	0.0119 (4)
O(64)		0.3026(2)	0.5555(2)	0.0259(2)	0.0096(4)

* U_{eq} is defined as one-third of the trace of the orthogonalized U_{ij} tensor.

Table 3: Interatomic distances (Å) for $Na_3SrMg_{11}(PO_4)_9$

(Sr,Na)(1)O$_9$	
SrNa(1)-O(44)	2.544(2) (×3)
SrNa(1)-O(31)	2.573(2) (×3)
SrNa(1)-O(33)	2.811(2) (×3)
<SrNa(1)-O>	**2.643(1)**
(Sr,Na)(2)O$_8$	
SrNa(2)-O(23)	2.404(2)
SrNa(2)-O(62)	2.500(2)
SrNa(2)-O(62)	2.537(2)
SrNa(2)-O(63)	2.621(2)
SrNa(2)-O(24)	2.679(2)
SrNa(2)-O(21)	2.692(2)
SrNa(2)-O(41)	2.724(2)
SrNa(2)-O(61)	2.801(1)
<SrNa(2)-O>	**2.619(1)**
Na(1)O$_6$	
Na(1)-O(53)	2.440(2) (×3)
Na(1)-O(31)	2.458(1) (×3)
<Na(1)-O>	**2.449(1)**
Na(2)O$_7$	
Na(2)-O(51)	2.322(2)
Na(2)-O(13)	2.468(1)
Na(2)-O(14)	2.474(1)
Na(2)-O(11)	2.481(2)
Na(2)-O(51)	2.523(2)
Na(2)-O(54)	2.698(1)
Na(2)-O(11)	2.726(1)
<Na(2)-O>	**2.527(1)**
Mg(1)O$_6$	
Mg(1)-O(21)	2.144(2) (×6)
<Mg(1)-O>	**2.144(2)**
Mg(2)O$_6$	
Mg(2)-O(11)	2.108(1) (×6)
<Mg(2)-O>	**2.108(1)**
Mg(3)O$_6$	
Mg(3)-O(22)	1.952(1) (×3)
Mg(3)-O(53)	2.167(2) (×3)
<Mg(3)-O>	**2.059(1)**
Mg(4)O$_6$	
Mg(4)-O(44)	2.040(1) (×3)
Mg(4)-O(64)	2.095(1) (×3)
<Mg(4)-O>	**2.067(1)**
Mg(5)O$_6$	
Mg(5)-O(12)	1.975(1) (×3)
Mg(5)-O(64)	2.178(2) (×3)
<Mg(5)-O>	**2.076(1)**
Mg(6)O$_5$	
Mg(6)-O(31)	1.972(1)
Mg(6)-O(51)	2.046(1)
Mg(6)-O(33)	2.077(2)
Mg(6)-O(14)	2.115(2)
Mg(6)-O(13)	2.255(1)
<Mg(6)-O>	**2.093(1)**
Mg(7)O$_5$	
Mg(7)-O(24)	2.042(1)
Mg(7)-O(44)	2.058(2)
Mg(7)-O(42)	2.065(1)
Mg(7)-O(33)	2.069(2)
Mg(7)-O(62)	2.120(1)
<Mg(7)-O>	**2.071(2)**
Mg(8)O$_5$	
Mg(8)-O(14)	2.001(1)
Mg(8)-O(24)	2.026(2)
Mg(8)-O(63)	2.032(1)
Mg(8)-O(52)	2.094(1)
Mg(8)-O(54)	2.191(2)
<Mg(8)-O>	**2.069(1)**
Mg(9)O$_5$	
Mg(9)-O(54)	1.983(2)
Mg(9)-O(32)	1.988(2)
Mg(9)-O(34)	2.009(2)
Mg(9)-O(53)	2.049(1)
Mg(9)-O(22)	2.235(1)
<Mg(9)-O>	**2.053(2)**
Mg(10)O$_6$	
Mg(10)-O(41)	1.948(2)
Mg(10)-O(43)	1.968(1)
Mg(10)-O(12)	2.022(1)
Mg(10)-O(61)	2.271(2)
Mg(10)-O(64)	2.321(1)
Mg(10)-O(63)	2.359(1)
<Mg(10)-O>	**2.148(1)**
Mg(11)O$_6$	
Mg(11)-O(61)	2.055(2)
Mg(11)-O(34)	2.063(1)
Mg(11)-O(23)	2.068(2)
Mg(11)-O(13)	2.094(1)
Mg(11)-O(52)	2.175(2)
Mg(11)-O(42)	2.241(1)
<Mg(11)-O>	**2.116(1)**
P(1)O$_4$	
P(1)-O(11)	1.506(2)
P(1)-O(12)	1.538(2)
P(1)-O(13)	1.547(1)
P(1)-O(14)	1.559(1)
<P(1)-O>	**1.537(1)**
P(2)O$_4$	
P(2)-O(21)	1.509(1)
P(2)-O(22)	1.527(1)
P(2)-O(23)	1.525(1)
P(2)-O(24)	1.584(1)
<P(2)-O>	**1.536(1)**
P(3)O$_4$	
P(3)-O(31)	1.526(2)
P(3)-O(32)	1.510(1)
P(3)-O(33)	1.551(1)
P(3)-O(34)	1.550(1)
<P(3)-O>	**1.534(1)**
P(4)O$_4$	
P(4)-O(41)	1.524(1)
P(4)-O(42)	1.535(1)
P(4)-O(43)	1.532(1)
P(4)-O(44)	1.550(2)
< P(4)-O>	**1.535(1)**
P(5)O$_4$	
P(5)-O(51)	1.521(2)
P(5)-O(52)	1.543(1)
P(5)-O(53)	1.545(1)
P(5)-O(54)	1.546(2)
<P(5)-O>	**1.539(2)**
P(6)O$_4$	
P(6)-O(61)	1.529(1)
P(6)-O(62)	1.535(1)
P(6)-O(63)	1.534(1)
P(6)-O(64)	1.540(2)
<P(6)-O>	**1.534(1)**

Table 4: Geometry parameters of the cationic sites in $Na_3SrMg_{11}(PO_4)_9$

$Na_{4/3}Ca_{4/3}Mg_7(PO_4)_6$ [3]				$Na_{2.5}Mg_7Y_{0.5}(PO_4)_6$ [6]				$Na_2Sr_{0.66}Mg_{7.33}(PO_4)_6$ This work			
Site	**n**	**<M–O> (Å)**	**BLD %**	**Site**	**n**	**<M–O> (Å)**	**BLD %**	**Site**	**n**	**<M–O> (Å)**	**BLD %**
Ca(1)	8	2.663	4.32	(Na,Y)	8	2.615	4.81	(Sr,Na)(2)	8	2.619	3.99
Ca(2)	6	2.324	0	Y(1)	6	2.226	0	Mg(1)	6	2.144	0
Ca(3)	6	2.208	0	Y(2)	6	2.206	0	Mg(2)	6	2.108	0
Na(1)	7	2.536	3.75	Na(1)	7	2.571	4.74	Na(2)	7	2.527	4.17
Na(2)	9	2.652	1.34	Na(2)	9	2.651	4.57	(Sr,Na)(1)	9	2.643	4.25
Na	-	-	-	Na(3)	6	2.432	0.22	Na(1)	6	2.449	0.37
Mg(1)	6	2.087	5.15	Mg(1)	6	2.074	5.3	Mg(3)	6	2.059	5.20
Mg(2)	6	2.056	1.77	Mg(2)	6	2.069	1.42	Mg(4)	6	2.067	1.33
Mg(3)	6	2.114	5.29	Mg(3)	6	2.081	3.43	Mg(5)	6	2.076	5.32
Mg(4)	6	2.141	8.45	Mg(4)	6	2.165	4.12	Mg(6)	5	2.093	3.52
Mg(5)	6	2.133	2.11	Mg(5)	6	2.124	2.68	Mg(7)	5	2.071	0.96
Mg(6)	5	2.088	7.03	Mg(6)	5	2.054	4.13	Mg(8)	5	2.069	2.85
Mg(7)	5	2.067	1.56	Mg(7)	5	2.08	1.02	Mg(9)	5	2.053	3.58
Mg(8)	5	2.075	3.03	Mg(8)	5	2.075	3.79	Mg(10)	6	2.148	7.86
Mg(9)	5	2.11	3.84	Mg(9)	5	2.089	3.59	Mg(11)	6	2.116	2.90
P(1)	4	1.534	0.49	P(1)	4	1.534	0.53	P(1)	4	1.537	1.04
P(2)	4	1.533	1.12	P(2)	4	1.533	0.94	P(2)	4	1.536	1.55
P(3)	4	1.532	1.33	P(3)	4	1.529	1.09	P(3)	4	1.534	1.06
P(4)	4	1.537	0.47	P(4)	4	1.54	0.32	P(4)	4	1.535	0.31
P(5)	4	1.536	0.42	P(5)	4	1.534	0.28	P(5)	4	1.539	0.57
P(6)	4	1.531	1.42	P(6)	4	1.536	0.73	P(6)	4	1.534	0.20

$BLD = \frac{100}{n} . \frac{\sum_{i=1}^{n} |M - O_i - < M - O >|}{< M - O >} \%$, where n is the number of bonds and (M–O) is the central cation-oxygene length.

Table 5: Assignment of observed ^{31}P chemical shifts and electric field strength (Z/a^2) to phosphate groups.

Signals	**Shift (ppm)**	**<Mg–O> (Å)**	**Z/a^2 ($Å^{-2}$)***	**Phosphate groups**
a	6.92	2.0297	0.48610	P(3)
b	3.68	2.0533	0.47725	P(4)
c	2.80	2.0778	0.46581	P(2)
d	1.77	2.0817	0.46387	P(1)
e	-0.38	2.101	0.45476	P(5)
f	-2.44	2.1789	0.42484	P(6)

* *Z*: the valence and *a*: the mean internuclear distance <Mg–O>